

# Dissipation-induced order: the $S = 1/2$ quantum spin chain coupled to an ohmic bath

Manuel Weber,<sup>1</sup> David J. Luitz,<sup>1</sup> and Fakher F. Assaad<sup>2,3</sup>

<sup>1</sup>Max Planck Institute for the Physics of Complex Systems, Nöthnitzer Str. 38, 01187 Dresden, Germany

<sup>2</sup>Institut für Theoretische Physik und Astrophysik, Universität Würzburg, 97074 Würzburg, Germany

<sup>3</sup>Würzburg-Dresden Cluster of Excellence ct.qmat, Am Hubland, 97074 Würzburg, Germany

(Dated: December 7, 2021)

We consider an  $S = 1/2$  antiferromagnetic quantum Heisenberg chain where each site is coupled to an independent bosonic bath with ohmic dissipation. The coupling to the bath preserves the global  $\text{SO}(3)$  spin symmetry. Using large-scale, approximation-free quantum Monte Carlo simulations, we show that any finite coupling to the bath suffices to stabilize long-range antiferromagnetic order. This is in stark contrast to the isolated Heisenberg chain where spontaneous symmetry breaking of the  $\text{SO}(3)$  symmetry is forbidden by the Mermin-Wagner theorem. A linear spin-wave theory analysis confirms that the memory of the bath and the concomitant retarded interaction stabilize the order. For the Heisenberg chain, the ohmic bath is a marginal perturbation so that exponentially large system sizes are required to observe long-range order at small couplings. Below this length scale, our numerics is dominated by a crossover regime where spin correlations show different power-law behaviors in space and time. We discuss experimental relevance of this crossover phenomena.

*Introduction.*—Real quantum systems are seldom isolated [1, 2]. The natural question to ask is if the coupling to the environment will trigger new phenomena, and, if so, at which energy or time scale. This question is not only relevant in the realm of quantum simulation or computing where decoherence is a limiting factor [3], but also in the solid state. A prominent example for this are experiments on  $\text{KCuF}_3$  [4], a quasi-one-dimensional material with weak inter-chain coupling. In this material, surrounding chains can be viewed as a weakly-coupled environment modifying the behavior of the chain: At *high* energies, neutron-scattering experiments are remarkably well reproduced by the two-spinon continuum of the isolated Heisenberg model; at *low* energies, the environment dominates, leading to the binding of spinons into spin waves.

One of our motivations is to understand the physics of chains of magnetic adatoms deposited on a metallic substrate [5]. Starting from an effective description of the magnetic adatoms in terms of a one-dimensional  $S = 1/2$  Heisenberg chain with a Kondo-type coupling to the substrate [6, 7], one can use Hertz-Millis theory [8, 9] to integrate out the bath and obtain in second-order perturbation theory a retarded interaction in space and time between the spin degrees of freedom. This interaction is governed by the spin susceptibility of the two-dimensional electron gas,  $\chi_0(i - j, \tau - \tau')$ , where  $i$  and  $j$  denote the positions of the magnetic adatoms and  $\tau, \tau'$  are points in imaginary time. It has a different decay in space (quartic) and time (quadratic). In our modeling, we will neglect the spatial decay since it is irrelevant at the Heisenberg critical point [10] and focus on the effect of retardation of the interaction in (imaginary) time [11, 12]. This allows us to simplify the model further and instead of a metallic substrate we introduce independent ohmic baths described by non-interacting bosons as in the celebrated Caldeira-Leggett model [13], leading to

the same retarded interaction in time if the bath is integrated out.

Spin chains in the presence of dissipation have been considered in the absence of the Berry phase, that renders the  $S = 1/2$  chain critical, within an  $\epsilon$ -expansion [14] as well as with Monte Carlo methods [15]. It was found that a finite coupling to the bath triggers a phase transition from a disordered phase at weak coupling to an ordered phase at strong coupling. This breakdown of the Mermin-Wagner theorem [16, 17] stems from the fact that the ohmic bath induces long-ranged retarded interactions. Calculations for the quantum XXZ chain with site ohmic dissipation coupling to the  $z$  component of the spin were carried out in Ref. [18].

In this Letter, we focus on the  $\text{SO}(3)$ -symmetric quantum Heisenberg chain with spin-symmetric coupling to the ohmic baths, fully taking into account the effects of the Berry phase. The recently introduced wormhole algorithm [19] permits positive-sign quantum Monte Carlo simulations for very large system sizes, which allows us to systematically study the approach towards the thermodynamic limit. We find that the coupling to the ohmic bath is marginal and that *any* coupling strength modifies the low-energy physics of the  $S = 1/2$  chain, stabilizing long-range antiferromagnetic order. Our results reveal a nontrivial finite length scale, separating suppressed correlations at short distances from the emergence of order at long distances. We expect that this length scale is observable in experiments for finite spin chains.

*Model.*—We consider the one-dimensional  $S = 1/2$  antiferromagnetic Heisenberg model

$$\hat{H}_s = J \sum_i \hat{\mathbf{S}}_i \cdot \hat{\mathbf{S}}_{i+1}, \quad (1)$$

where we use the exchange coupling  $J = 1$  as the unit of energy. Its ground state shows critical antiferromagnetic correlations given for long distances by  $C(r) = \langle \hat{S}_0^z \hat{S}_r^z \rangle \propto$

$(-1)^r (\ln r)^{1/2} r^{-1}$ , where the power law is tied to the global SO(3) spin symmetry [20].

To study the effects of dissipation on the Heisenberg chain, we introduce an independent bosonic bath coupled to each spin component  $\hat{S}_i^\alpha$ . The total Hamiltonian is given by  $\hat{H} = \hat{H}_s + \hat{H}_{\text{sb}}$ , with

$$\hat{H}_{\text{sb}} = \sum_{iq} \omega_q \hat{\mathbf{a}}_{iq}^\dagger \cdot \hat{\mathbf{a}}_{iq} + \sum_{iq} \lambda_q (\hat{\mathbf{a}}_{iq}^\dagger + \hat{\mathbf{a}}_{iq}) \cdot \hat{\mathbf{S}}_i. \quad (2)$$

Here,  $\hat{\mathbf{a}}_{iq}^\dagger, \hat{\mathbf{a}}_{iq}$  are 3-component vectors of bosonic creation and annihilation operators. The bath consists of a continuum of modes  $q$  with frequency  $\omega_q$  and spin-boson coupling  $\lambda_q$ . Our model satisfies the global SO(3) rotational symmetry generated by the total angular momentum  $\hat{\mathbf{J}}_{\text{tot}} = \sum_{iq} \hat{\mathbf{Q}}_{iq} \times \hat{\mathbf{P}}_{iq} + \sum_i \hat{\mathbf{S}}_i$ , where  $\hat{\mathbf{Q}}_{iq} = \frac{1}{\sqrt{2}}(\hat{\mathbf{a}}_{iq}^\dagger + \hat{\mathbf{a}}_{iq})$  and  $\hat{\mathbf{P}}_{iq} = \frac{i}{\sqrt{2}}(\hat{\mathbf{a}}_{iq}^\dagger - \hat{\mathbf{a}}_{iq})$  are the bosonic position and momentum operators, respectively. The effects of the bath on the spin system are fully determined by the spectral density  $J(\omega) = \pi \sum_q \lambda_q^2 \delta(\omega - \omega_q)$ . An ohmic bath corresponds to a power-law spectrum

$$J(\omega) = 2\pi\alpha J^{1-s}\omega^s, \quad 0 < \omega < \omega_c, \quad (3)$$

with exponent  $s = 1$  [1]. Here, we introduced the dimensionless coupling constant  $\alpha$  and the frequency cutoff  $\omega_c$ .

The bath can be integrated out exactly and the partition function  $Z = Z_b \text{Tr}_s \hat{\mathcal{T}}_\tau e^{-\hat{\mathcal{H}}}$  is fully determined by the spin subsystem  $\hat{\mathcal{H}} = \hat{\mathcal{H}}_s + \hat{\mathcal{H}}_{\text{ret}}$ . The spin-boson coupling in Eq. (2) leads to a retarded spin-spin interaction

$$\hat{\mathcal{H}}_{\text{ret}} = - \iint_0^\beta d\tau d\tau' \sum_i K(\tau - \tau') \hat{\mathbf{S}}_i(\tau) \cdot \hat{\mathbf{S}}_i(\tau'), \quad (4)$$

which encodes the memory of the bath. It is mediated by the bath propagator

$$K(\tau) = \int_0^{\omega_c} d\omega \frac{J(\omega)}{\pi} \frac{\cosh[\omega(\beta/2 - \tau)]}{2 \sinh[\omega\beta/2]}, \quad (5)$$

where  $0 \leq \tau < \beta$  and  $K(\tau + \beta) = K(\tau)$ . Here,  $\beta = 1/T$  is the inverse temperature. The power-law spectrum in Eq. (3) yields  $K(\tau) \sim 1/\tau^{1+s}$  for  $\omega_c\tau \gg 1$ .

The retarded interaction can invalidate the Mermin-Wagner theorem and produce long-range order even in one spatial dimension. In the Supplemental Material (SM) [21], we provide a linear spin-wave theory analysis of our model, which shows that at large  $S$  spin waves do not destabilize antiferromagnetic long-range order in the presence of dissipation. Further insight comes from considering the isolated spin chain, and, at this critical point, computing the scaling dimension of the retarded interaction. One obtains  $\Delta = 1 - s$  such that the ohmic case,  $s = 1$ , is marginal [22, 23]. The goal here is to investigate numerically if the coupling is marginally relevant or irrelevant.

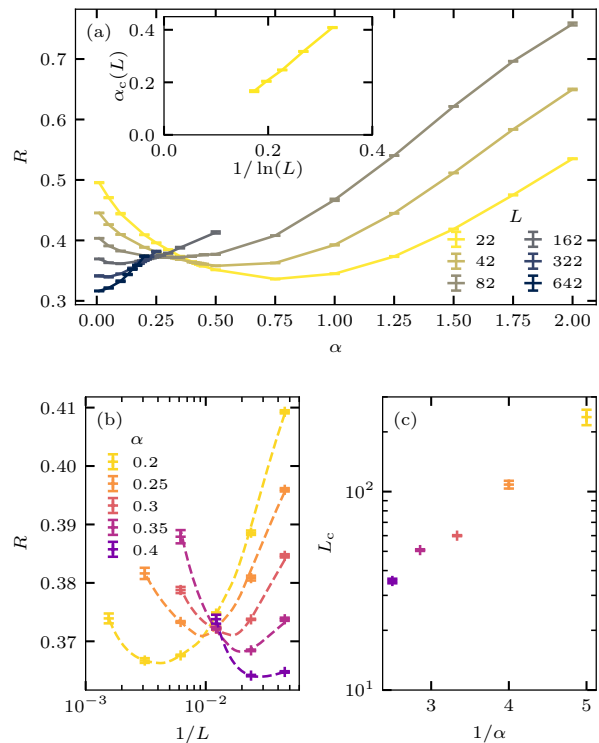


FIG. 1. (a) Antiferromagnetic correlation ratio  $R$  as a function of the spin-boson coupling  $\alpha$  for different system sizes  $L$ . A finite-size scaling of the crossings  $\alpha_c(L)$  between data pairs  $\{L, 2L - 2\}$  is shown as an inset. (b)  $R(1/L)$  for different  $\alpha$ . The minima of  $R(1/L)$  define a crossover scale  $L_c(\alpha)$  beyond which  $R$  increases.  $L_c$  is estimated using spline fits and shown in (c). The crossover scale is consistent with an exponential scaling  $L_c \propto \exp(\xi/\alpha)$ .

*Method.*—For our simulations, we used an exact quantum Monte Carlo method for retarded interactions [24] that samples a diagrammatic expansion of  $Z/Z_b$  in  $\hat{\mathcal{H}}_s + \hat{\mathcal{H}}_{\text{ret}}$ . Our approach is based on the stochastic series expansion [25] with global directed-loop updates [26] and makes use of efficient wormhole moves [19] recently developed for retarded spin-flip interactions as in Eq. (4). The time dependence of  $K(\tau - \tau')$  only enters during the diagonal updates and is sampled exactly using inverse transform sampling [19]; we set  $\omega_c/J = 10$ , similar to Ref. [18]. At  $\alpha = 0$ , Lorentz invariance guarantees convergence to the ground state at inverse temperatures  $\beta \propto L$ . This is no longer true for  $\alpha > 0$ , so that we ensure convergence in temperature for all results, as demonstrated in the SM [21]. For the largest system sizes we reach  $\beta J \approx 10.000$  and we use periodic boundary conditions. For a detailed description of our method see Ref. [19].

*Results.*—To probe for long-range order, we compute the equal-time spin structure factor defined as

$$S(q) = \frac{1}{L} \sum_{ij} e^{iq(i-j)} \langle \hat{S}_i^z \hat{S}_j^z \rangle. \quad (6)$$

Owing to the spin-rotational symmetry of our model, it is sufficient to consider only the  $z$  component of the spin. We also calculate the correlation ratio [27, 28],

$$R = 1 - \frac{S(Q + \delta q)}{S(Q)}, \quad (7)$$

at the ordering momentum  $Q = \pi$  and with resolution  $\delta q = 2\pi/L$ , as it is particularly useful to detect quantum phase transitions:  $R$  scales to unity (zero) in the ordered (disordered) phase and corresponds to a renormalization-group-invariant quantity at criticality. Figure 1(a) shows temperature-converged results of  $R$  for each chain length  $L$  and coupling strength  $\alpha$ . For *large* values of  $\alpha$ , the correlation ratio grows, thus lending support to long-range antiferromagnetic order as suggested by linear spin-wave theory [21]. To understand the limit of strong bath coupling  $\alpha$ , we consider  $J = 0$  in Eq. (1). In this case,  $\hat{\mathbf{J}}_{i,\text{tot}} = \sum_q \hat{\mathbf{Q}}_{iq} \times \hat{\mathbf{P}}_{iq} + \hat{\mathbf{S}}_i$  is a good quantum number such that the ground state for each site, consisting of a spin and the bath, has a half-integer angular momentum and is hence at least two-fold degenerate, i.e., the bath cannot screen the spin degree of freedom. This leads to a macroscopic degeneracy, which is lifted at finite  $J$  by the onset of long ranged order, as shown in Fig. 1(a).

We now turn our attention to the weak-coupling limit. Considering pairs of chain lengths, we observe that the crossing of  $R(\alpha, L)$  and  $R(\alpha, 2L - 2)$  at  $\alpha_c(L)$  systematically drifts to lower values of  $\alpha$ . As apparent from the inset of Fig. 1(a) and for our considered lattice sizes,  $\alpha_c(L) \simeq 1/\ln(L)$ . Figure 1(b) shows the correlation ratio  $R$  at fixed coupling  $\alpha$  and as a function of lattice size, revealing a characteristic length scale  $L_c$  at which  $R$  shows a minimum. The  $\alpha$  dependence of  $L_c$ , shown in Fig. 1(c), is consistent with an exponential law,  $L_c(\alpha) \propto e^{\xi/\alpha}$ , suggesting that the coupling to the ohmic bath is marginally relevant. As a consequence, exponentially large lattices are required to observe ordering in the regime of small  $\alpha$ .

The length scale  $L_c$ , beyond which the correlation ratio  $R$  grows, is revealed by the real-space correlations  $C(r)$  shown in Fig. 2. At  $\alpha = 0.1$ , this length scale lies beyond the lattice sizes accessible in our simulations, and  $C(r)$  is, up to an overall scaling factor, not distinguishable from the correlations in the Heisenberg model. We interpret the renormalization of the short-ranged spin-spin correlations in terms of entanglement between bath and spin degrees of freedom. At  $\alpha = 0.25$ , the correlation ratio grows for  $L \gtrsim 82$ , as can be seen in Fig. 1(b). The length scale  $L_c$  marks a distinct departure from the Heisenberg scaling and a levelling off of the spin-spin correlations in Fig. 2. Ultimately for  $\alpha \geq 1$ ,  $L_c$  drops below our smallest system size, the Heisenberg scaling is not apparent any more, and the data clearly supports long-ranged order. We also note that while initially decreasing, the magnitude of the short-ranged spin-spin correlations grows for *large* values of  $\alpha$ .

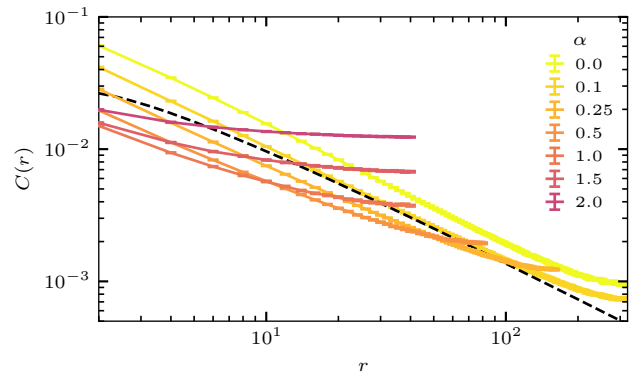


FIG. 2. Real-space correlation function  $C(r)$  for even  $r$  at the largest available  $L \in \{82, 162, 322, 642\}$  for different  $\alpha$ . For  $\alpha = 0$ , the exact asymptotic form (dashed line),  $C(r) \sim (-1)^r (\ln r)^{1/2} / [(2\pi)^{3/2} r]$ , is approached very slowly [20]. A finite-size analysis of the boundary effects near  $r = L/2$  can be found in the SM [21].

Figure 3 displays the spin structure factor  $S(q)$  as well as the square of the antiferromagnetic order parameter,

$$m^2(L) = \frac{1}{L} S(q = \pi). \quad (8)$$

In the absence of the bath,  $S(q = \pi)$  diverges logarithmically [Fig. 3(a)] so that  $m^2(L \rightarrow \infty)$  vanishes [Fig. 3(c)]. For *large* bath couplings  $\alpha$ , we observe a finite order parameter  $m^2(L \rightarrow \infty) > 0$  in Fig. 3(c), in accordance with our analysis of the correlation ratio. At small  $\alpha$ , distinguishing  $m^2(L \rightarrow \infty)$  from zero becomes challenging. In this limit, the data of Fig. 2 show that the spin-spin correlations decay as  $1/r$  for  $r < L_c$  before leveling off. Hence,

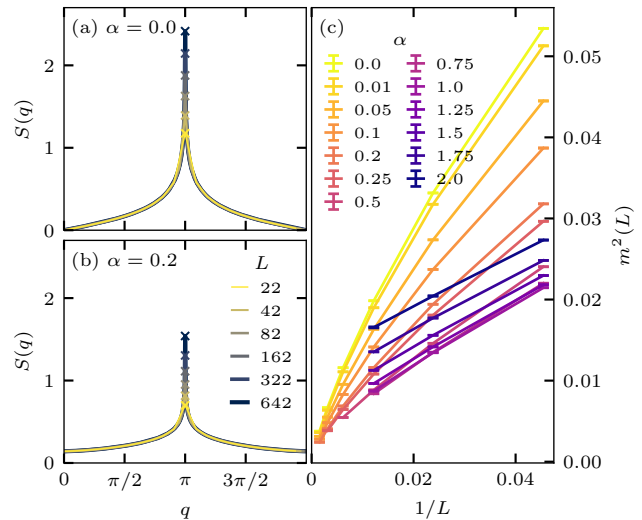


FIG. 3. Finite-size dependence of the spin structure factor  $S(q)$  for (a)  $\alpha = 0.0$  and (b)  $\alpha = 0.2$ . (c) Finite-size scaling of the order parameter  $m^2(L) = S(q = \pi)/L$  for different  $\alpha$ .

we conjecture that  $\lim_{L \rightarrow \infty} m^2(L) \propto 1/L_c(\alpha) \propto e^{-\xi/\alpha}$ . The structure factor equally reveals the value of the total spin via  $S(q=0) = \frac{1}{L} (\sum_i \hat{S}_i)^2$ . For the Heisenberg chain, the total spin is a good quantum number and vanishes at zero temperature on any finite lattice [Fig. 3(a)], whereas any nonzero coupling to the bath breaks this symmetry [Fig. 3(b)]. The finite value of  $S(q=0)$  reflects the entanglement of the spin chain and the bath.

From the equal-time correlation functions, one would conclude that in the small  $\alpha$  limit and at distances smaller than  $L_c$  one observes the physics of the Heisenberg model. This turns out not to be the case. One of the defining properties of the Heisenberg chain is Lorentz invariance that renders space and time interchangeable. In Fig. 4 we show the local spin susceptibility

$$\chi(r=0, L, \beta) = \frac{1}{L} \sum_{i=1}^L \int_0^\beta d\tau \langle \hat{S}_i^z(\tau) \hat{S}_i^z(0) \rangle \quad (9)$$

where  $\hat{S}_i^z(\tau) = e^{\tau \hat{H}} \hat{S}_i^z e^{-\tau \hat{H}}$ . As detailed in the SM [21], for the Heisenberg model  $\chi(r=0, L, \beta \rightarrow \infty) \propto \ln(L)$  and  $\chi(r=0, L \rightarrow \infty, \beta) \propto \ln(\beta)$ . In Fig. 4(a) this scaling is confirmed for the Heisenberg model. Of particular interest is the data set at  $\alpha = 0.1$ . Here, our lattice sizes are smaller than  $L_c(\alpha)$  and the real-space correlations  $C(r)$  in Fig. 2 are not distinguishable from those of the Heisenberg model. However,  $\chi(r=0)$  shows marked deviations from the logarithmic scaling of the Heisenberg model. Hence, in the crossover regime where our system sizes are smaller than  $L_c(\alpha)$ , the local susceptibility is not controlled by the Heisenberg fixed point. In particular, our data is consistent with correlations in time that decay slower than  $1/\tau$ . For larger values of  $\alpha$  our system sizes exceed  $L_c$  such that we can pick up long-range order in the local susceptibility, i.e.,  $\chi(r=0, L \rightarrow \infty, \beta) \propto \beta$ . As apparent from Fig. 4(b), we observe this behavior for large values of  $\alpha$ . Note that for any value of  $\alpha$  we expect the local susceptibility to reveal long-range order for lattice sizes  $L > L_c(\alpha)$ .

*Discussion.*—Our results demonstrate the efficiency of our quantum Monte Carlo method for retarded interactions. Unprecedentedly large lattices at very low temperatures can be reached, necessary to reveal the physics of dissipative  $S = 1/2$  quantum spin chains.

To at best interpret our results, it is convenient to consider our model in the  $\alpha$  versus  $s$  plane. For  $s < 1$  ( $s > 1$ ) the coupling to the bath is relevant (irrelevant). For  $s > 1$  we conjecture that there will be a phase transition between the Heisenberg chain and a phase with long-ranged order at finite value of  $\alpha_c(s)$ . We note that for the 1+1 dimensional non-linear Ising and  $O(2)$  sigma models, such a dissipation induced ordering transition has been studied [15]. At  $s = 1$  (considered here), the coupling to the bath is marginal, and our results are consistent with the interpretation that it is *marginally relevant*. As a consequence, we observe a very slow flow: in

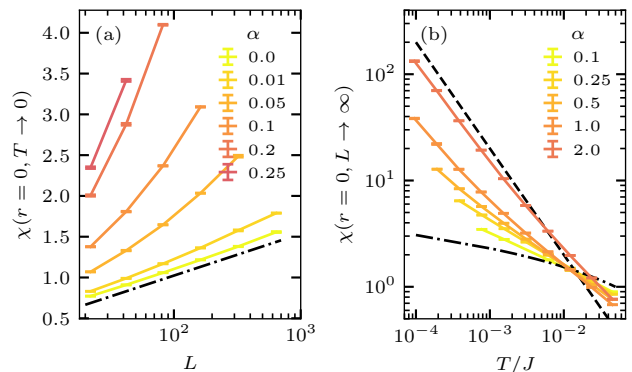


FIG. 4. Local spin susceptibility  $\chi(r=0)$  (a) for  $T \rightarrow 0$  as a function of  $L$  and (b) for  $L \rightarrow \infty$  as a function of  $T$ . The dot-dashed lines indicate an  $\ln L$  dependence in (a) and an  $\ln \beta$  dependence in (b), whereas the dashed line in (b) corresponds to the  $\chi \sim 1/T$  behavior expected for the ordered state.

the small  $\alpha$  regime lattice sizes greater than  $L_c(\alpha) \propto e^{\xi/\alpha}$  are required to reveal long range ordering. The physics in the crossover regime  $L < L_c(\alpha)$  is particularly interesting. Here, the real-space correlation functions decay as  $1/r$  akin to the Heisenberg chain. On the other hand, the imaginary-time correlations reveal a breakdown of Lorentz invariance and fall off much slower than  $1/\tau$ . A possible interpretation is the proximity to the quantum phase transition at  $\alpha_c(s)$  for  $s > 1$ . As seen in Ref. [15] for the 1+1 dimensional non-linear  $O(n)$  sigma models, such transitions have dynamical exponents  $z > 1$  with  $\tau^{-1/z}$  decay in imaginary time. Such an interpretation of the data can be tested since the phase diagram of our model in the  $\alpha$ - $s$  plane can be investigated with our quantum Monte Carlo algorithm.

Our model is relevant for the understanding of chains of magnetic adatoms on two-dimensional metallic surfaces [5]. These experiments are typically limited to a small number of adatoms. The fact that the coupling to the bath is marginally relevant implies that the physics of these chains will be captured by the crossover regime. Furthermore, spin-orbit coupling, generically present at surfaces, will break the  $SO(3)$  spin symmetry down to  $SO(2)$ . Similar calculations as presented here but for the XXZ chain are hence of particular interest.

The finite-temperature and dynamical properties of our model will reveal how the two-spinon continuum will evolve when coupled to the bath. While the high-energy features of the dynamical spin structure factor will reveal the two-spinon continuum, the low-energy features should be captured by the spin-wave theory [21] of damped magnons with spectral weight emerging above  $\omega \propto k^2$ .

We thank B. Danu, T. Grover and M. Vojta for many illuminating discussions on related research. FFA thanks the DFG for funding via the Würzburg-Dresden Clus-

ter of Excellence on Complexity and Topology in Quantum Matter ct.qmat (EXC 2147, project-id 390858490). DJL acknowledges support by the DFG through SFB 1143 (project-id 247310070) and the cluster of excellence ML4Q (EXC2004, project-id 390534769).

- 
- [1] U. Weiss, *Quantum Dissipative Systems*, edited by I. Dzyaloshinski and Y. Lu, Series in modern condensed matter physics (World Scientific, 2008).
- [2] H.-P. Breuer and F. Petruccione, *The Theory of Open Quantum Systems* (Oxford University Press, 2002).
- [3] J. Preskill, Quantum Computing in the NISQ era and beyond, *Quantum* **2**, 79 (2018).
- [4] B. Lake, D. A. Tennant, C. D. Frost, and S. E. Nagler, Quantum criticality and universal scaling of a quantum antiferromagnet, *Nat Mater* **4**, 329 (2005).
- [5] R. Toskovic, R. van den Berg, A. Spinelli, I. S. Eliens, B. van den Toorn, B. Bryant, J. S. Caux, and A. F. Otte, Atomic spin-chain realization of a model for quantum criticality, *Nature Physics* **12**, 656 EP (2016).
- [6] B. Danu, F. F. Assaad, and F. Mila, Exploring the Kondo Effect of an Extended Impurity with Chains of Co Adatoms in a Magnetic Field, *Phys. Rev. Lett.* **123**, 176601 (2019).
- [7] B. Danu, M. Vojta, F. F. Assaad, and T. Grover, Kondo Breakdown in a Spin-1/2 Chain of Adatoms on a Dirac Semimetal, *Phys. Rev. Lett.* **125**, 206602 (2020).
- [8] J. A. Hertz, Quantum critical phenomena, *Phys. Rev. B* **14**, 1165 (1976).
- [9] A. J. Millis, Effect of a nonzero temperature on quantum critical points in itinerant fermion systems, *Phys. Rev. B* **48**, 7183 (1993).
- [10] Power counting shows that interactions decaying with a quartic power law are irrelevant at the Heisenberg critical point [22, 23].
- [11] A. M. Lobos, M. A. Cazalilla, and P. Chudzinski, Magnetic phases in the one-dimensional Kondo chain on a metallic surface, *Phys. Rev. B* **86**, 035455 (2012).
- [12] A. J. Friedman, Dissipative Luttinger liquids (2019), [arXiv:1910.06371 \[cond-mat.quant-gas\]](https://arxiv.org/abs/1910.06371).
- [13] A. O. Caldeira and A. J. Leggett, Influence of dissipation on quantum tunneling in macroscopic systems, *Phys. Rev. Lett.* **46**, 211 (1981).
- [14] S. Pankov, S. Florens, A. Georges, G. Kotliar, and S. Sachdev, Non-fermi-liquid behavior from two-dimensional antiferromagnetic fluctuations: A renormalization-group and large- $n$  analysis, *Phys. Rev. B* **69**, 054426 (2004).
- [15] P. Werner, M. Troyer, and S. Sachdev, Quantum spin chains with site dissipation, *Journal of the Physical Society of Japan* **74**, 67 (2005), <https://doi.org/10.1143/JPSJS.74S.67>.
- [16] N. D. Mermin and H. Wagner, Absence of Ferromagnetism or Antiferromagnetism in One- or Two-Dimensional Isotropic Heisenberg Models, *Phys. Rev. Lett.* **17**, 1133 (1966).
- [17] P. C. Hohenberg, Existence of Long-Range Order in One and Two Dimensions, *Phys. Rev.* **158**, 383 (1967).
- [18] Z. Cai, U. Schollwöck, and L. Pollet, Identifying a Bath-Induced Bose Liquid in Interacting Spin-Boson Models, *Phys. Rev. Lett.* **113**, 260403 (2014).
- [19] M. Weber, Quantum Monte Carlo simulation of spin-boson models using wormhole updates (2021), [arXiv:2108.01131 \[cond-mat.str-el\]](https://arxiv.org/abs/2108.01131).
- [20] I. Affleck, Exact correlation amplitude for the Heisenberg antiferromagnetic chain, *Journal of Physics A: Mathematical and General* **31**, 4573 (1998).
- [21] See Supplemental Material at [URL].
- [22] J. Cardy, *Scaling and Renormalization in Statistical Physics*, Cambridge Lecture Notes in Physics (Cambridge University Press, 1996).
- [23] N. Goldenfeld, *Lectures on Phase Transitions and the Renormalization Group (1st ed.)* (CRC Press, (1992)).
- [24] M. Weber, F. F. Assaad, and M. Hohenadler, Directed-Loop Quantum Monte Carlo Method for Retarded Interactions, *Phys. Rev. Lett.* **119**, 097401 (2017).
- [25] A. W. Sandvik and J. Kurkijärvi, Quantum Monte Carlo simulation method for spin systems, *Phys. Rev. B* **43**, 5950 (1991).
- [26] O. F. Syljuåsen and A. W. Sandvik, Quantum Monte Carlo with directed loops, *Phys. Rev. E* **66**, 046701 (2002).
- [27] A. W. Sandvik, Computational Studies of Quantum Spin Systems, *AIP Conference Proceedings* **1297**, 135 (2010), <https://aip.scitation.org/doi/pdf/10.1063/1.3518900>.
- [28] R. K. Kaul, Spin nematics, valence-bond solids, and spin liquids in  $SO(n)$  quantum spin models on the triangular lattice, *Phys. Rev. Lett.* **115**, 157202 (2015).
- [29] J. W. Negele and H. Orland, *Quantum Many-Particle Systems* (Perseus Books, Reading, MA, 1998).

## Supplemental Material

for

### Dissipation-induced order: the $S = 1/2$ quantum spin chain coupled to an ohmic bath

#### FINITE-TEMPERATURE ANALYSIS OF THE ORDER PARAMETER

Figure S1 shows the inverse-temperature dependence of the order parameter  $S(\pi)$  and the correlation ratio  $R$  for different spin-boson couplings  $\alpha$  and different system sizes  $L$ . To determine the ground-state properties of the dissipative Heisenberg chain, we have to make sure that our observables are converged for each parameter set. For  $\alpha = 0$ , it is sufficient to choose inverse temperatures  $\beta = 2L$  to get converged results and we reach system sizes up to  $L = 642$ . Here, the  $\beta \sim L^z$  scaling with dynamical exponent  $z = 1$  is a consequence of conformal invariance. The coupling to the bath breaks conformal invariance so that we have to simulate at increasingly lower temperatures with increasing  $\alpha$  and  $L$ . For the strongest couplings  $\alpha = 1.0$  or  $2.0$ , we can only reach temperature convergence up to  $L = 82$  where  $\beta J/L \approx 2^7$  ( $\beta J \approx 10.000$ ) is required. Moreover, when doubling the system sizes in Figs. S1(d), S1(e), S1(i), and S1(j) we approximately need an additional factor of 2 in  $\beta/L$  for temperature convergence. This is a strong hint towards  $z = 2$  scaling, as predicted by our spin-wave calculation (see below). At smaller couplings, we also expect a crossover toward  $z = 2$  scaling, but system sizes are still too small to resolve this. The temperature dependence of  $S(\pi)$  and  $R$  in Fig. S1 is representative for other equal-time observables.

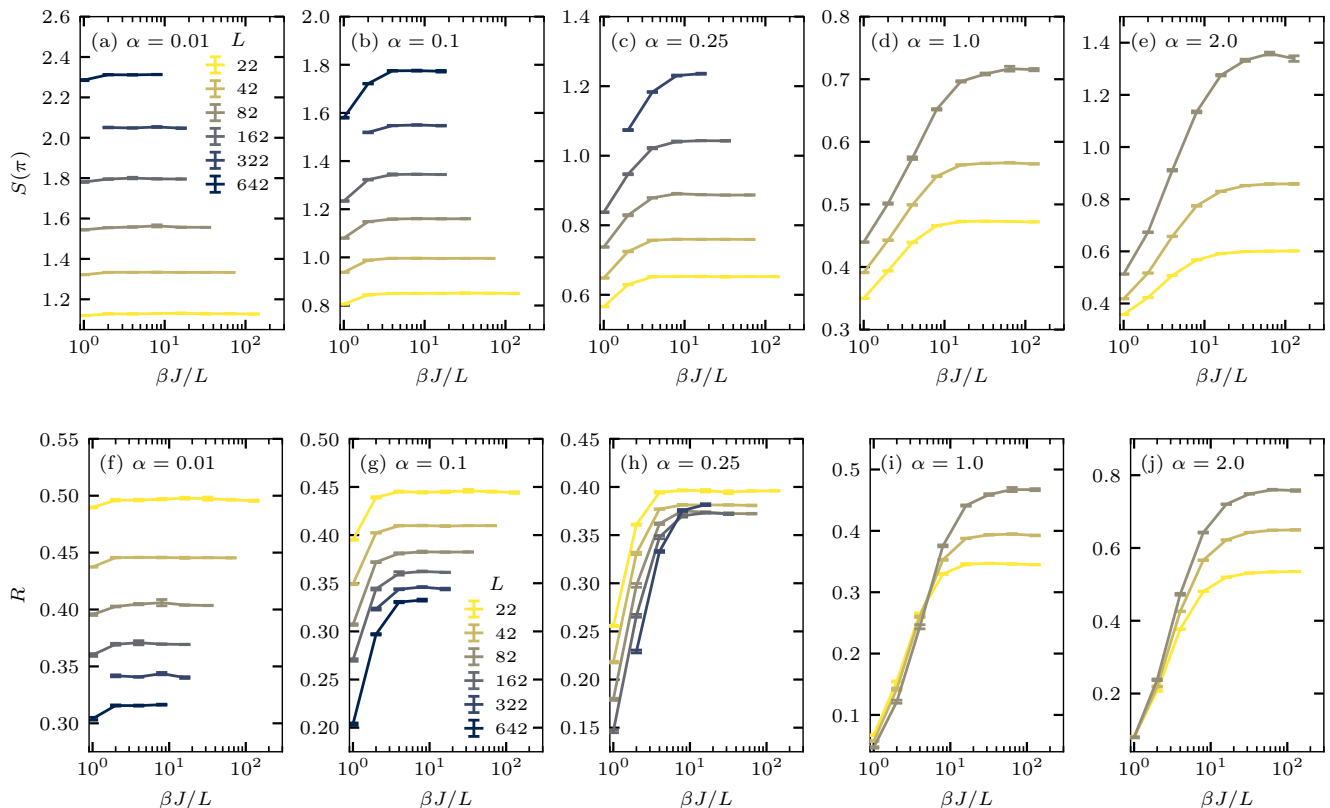


FIG. S1. Convergence of (a)–(e) the order parameter  $S(\pi)$  and (f)–(j) the correlation ratio  $R$  as a function of  $\beta/L$  for different spin-boson couplings  $\alpha$  and lattice sizes  $L$ . We have chosen all data points according to  $\beta/L = 2^n$ ,  $n \in \mathbb{N}_0$ .

## FINITE-SIZE DEPENDENCE OF THE REAL-SPACE CORRELATIONS

Figure S2 shows a finite-size analysis of the real-space spin-spin correlation function  $C(r)$  for different couplings  $\alpha$ . In the absence of conformal invariance, we cannot use the conformal distance to get rid of boundary effects. Therefore, we have to analyze  $C(r)$  for different  $L$  to estimate the maximum distance  $r$  that has already converged to the  $L \rightarrow \infty$  limit. For a detailed discussion of  $C(r)$  we refer to the main part of our paper.

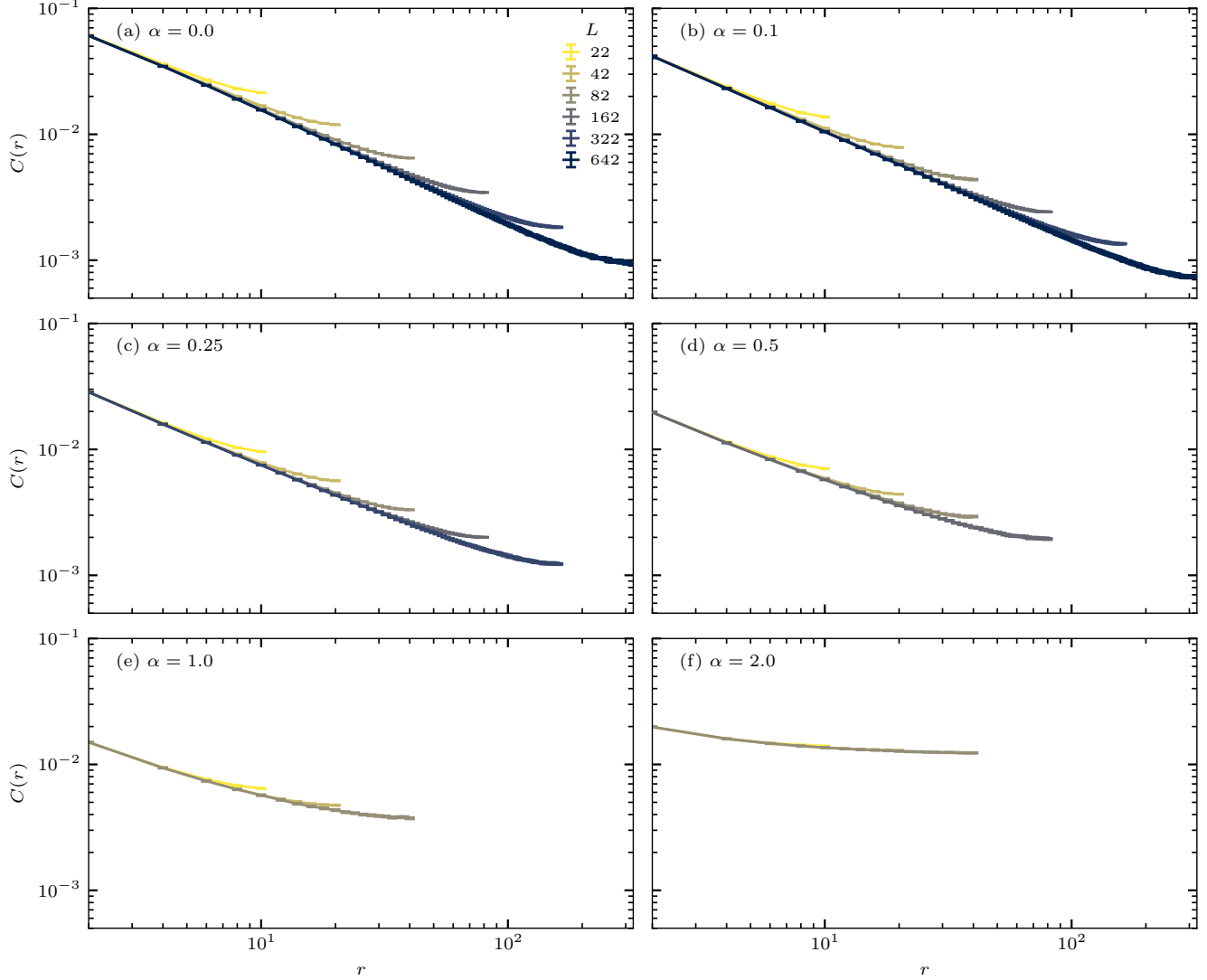


FIG. S2. Finite-size dependence of the real-space spin-spin correlation function  $C(r)$  for different spin-boson couplings  $\alpha$ . For each lattice size  $L$ ,  $C(r)$  has converged to the zero-temperature result according to Fig. S1.

## LINEAR SPIN-WAVE THEORY FOR THE DISSIPATIVE HEISENBERG ANTIFERROMAGNET

In the following, we perform the linear spin-wave approximation for the antiferromagnetic Heisenberg model coupled to a bosonic bath. We consider the Hamiltonian  $\hat{H} = \hat{H}_s + \hat{H}_{\text{sb}}$  with

$$\hat{H}_s = J \sum_{\langle ij \rangle} \hat{\mathbf{S}}_i \cdot \hat{\mathbf{S}}_j, \quad (\text{S1})$$

$$\hat{H}_{\text{sb}} = \sum_{iq} \omega_q \hat{\mathbf{a}}_{iq}^\dagger \cdot \hat{\mathbf{a}}_{iq} + \sum_{iq} \lambda_q (\hat{\mathbf{a}}_{iq}^\dagger + \hat{\mathbf{a}}_{iq}) \cdot \hat{\mathbf{S}}_i. \quad (\text{S2})$$

### Holstein-Primakoff transformation

First, we use the Holstein-Primakoff transformation to represent the spins in terms of bosonic operators. We assume that the model is defined on a bipartite lattice. On sublattice A, we expand around the spin- $S$  state in  $z$  direction, i.e.,

$$i \in \text{sublattice A:} \quad \hat{S}_i^z = S - \hat{A}_i^\dagger \hat{A}_i, \quad (\text{S3})$$

$$\hat{S}_i^+ = \sqrt{2S - \hat{A}_i^\dagger \hat{A}_i} \hat{A}_i = \sqrt{2S} \hat{A}_i + \mathcal{O}(S^{-1/2}), \quad (\text{S4})$$

$$\hat{S}_i^- = \hat{A}_i^\dagger \sqrt{2S - \hat{A}_i^\dagger \hat{A}_i} = \sqrt{2S} \hat{A}_i^\dagger + \mathcal{O}(S^{-1/2}), \quad (\text{S5})$$

whereas on sublattice B we expand around  $-S$ , i.e.,

$$j \in \text{sublattice B:} \quad \hat{S}_j^z = \hat{B}_j^\dagger \hat{B}_j - S, \quad (\text{S6})$$

$$\hat{S}_j^+ = \hat{B}_j^\dagger \sqrt{2S - \hat{B}_j^\dagger \hat{B}_j} = \sqrt{2S} \hat{B}_j^\dagger + \mathcal{O}(S^{-1/2}), \quad (\text{S7})$$

$$\hat{S}_j^- = \sqrt{2S - \hat{B}_j^\dagger \hat{B}_j} \hat{B}_j = \sqrt{2S} \hat{B}_j + \mathcal{O}(S^{-1/2}). \quad (\text{S8})$$

Note that we have approximated the spin flip operators in such a way that our final result will be correct up to  $\mathcal{O}(S^0)$  corrections. For the contribution of the system, we obtain the familiar result for the antiferromagnetic Heisenberg model,

$$\hat{H}_s = \frac{LqJS^2}{2} + JS \sum_{\langle i,j \rangle} (\hat{A}_i \hat{B}_j + \hat{A}_i^\dagger \hat{B}_j^\dagger) + qJS \sum_{i \in \text{A}} \hat{A}_i^\dagger \hat{A}_i + qJS \sum_{j \in \text{B}} \hat{B}_j^\dagger \hat{B}_j + \mathcal{O}(S^0), \quad (\text{S9})$$

where  $q$  is the coordination number of the lattice. Note that we drop all  $\mathcal{O}(S^0)$  terms. The spin-boson part becomes

$$\begin{aligned} \hat{H}_{\text{sb}} = & \sum_{iq} \omega_q \hat{\mathbf{a}}_{iq}^\dagger \cdot \hat{\mathbf{a}}_{iq} + \sum_{i \in \text{A}} \sum_q \lambda_q (\hat{\mathbf{a}}_{iq}^\dagger + \hat{\mathbf{a}}_{iq}) \cdot \begin{pmatrix} \sqrt{S/2} [\hat{A}_i^\dagger + \hat{A}_i] \\ i\sqrt{S/2} [\hat{A}_i^\dagger - \hat{A}_i] \\ S - \hat{A}_i^\dagger \hat{A}_i \end{pmatrix} \\ & + \sum_{j \in \text{B}} \sum_q \lambda_q (\hat{\mathbf{a}}_{jq}^\dagger + \hat{\mathbf{a}}_{jq}) \cdot \begin{pmatrix} \sqrt{S/2} [\hat{B}_j + \hat{B}_j^\dagger] \\ i\sqrt{S/2} [\hat{B}_j - \hat{B}_j^\dagger] \\ \hat{B}_j^\dagger \hat{B}_j - S \end{pmatrix} + \mathcal{O}(S^{-1/2}). \end{aligned} \quad (\text{S10})$$

At this stage, it is still important to keep the  $\mathcal{O}(S^0)$  term in the spin- $z$  component of  $\hat{H}_{\text{sb}}$ .

### Integrating out the bosonic bath in the path-integral formulation

Second, we introduce the coherent-state path integral for the partition function,

$$Z = \int \mathcal{D}(\bar{A}, A) \int \mathcal{D}(\bar{B}, B) e^{-\mathcal{S}_s[\bar{A}, A, \bar{B}, B]} \int \mathcal{D}(\bar{\mathbf{a}}, \mathbf{a}) e^{-\mathcal{S}_{\text{sb}}[\bar{A}, A, \bar{B}, B, \bar{\mathbf{a}}, \mathbf{a}]}, \quad (\text{S11})$$



where we represent all operators in terms of bosonic coherent states. Here,  $\mathcal{S}_s$  and  $\mathcal{S}_{sb}$  are the actions that correspond to Eqs. (S9) and (S10), respectively. For details on coherent states and the path-integral formalism, see Ref. [29]. In a third step, we integrate out the bosonic bath and obtain

$$Z = Z_b \int \mathcal{D}(\bar{A}, A) \int \mathcal{D}(\bar{B}, B) e^{-\mathcal{S}_s[\bar{A}, A, \bar{B}, B] - \mathcal{S}_{ret}[\bar{A}, A, \bar{B}, B]}, \quad (\text{S12})$$

where  $Z_b$  is the partition function of the noninteracting bath. The contribution of the system to the action is given by

$$\begin{aligned} \mathcal{S}_s = & \frac{L\beta qJS^2}{2} + JS \int_0^\beta d\tau \sum_{\langle i,j \rangle} [A_i(\tau) B_j(\tau) + \bar{A}_i(\tau) \bar{B}_j(\tau)] \\ & + \int_0^\beta d\tau \left[ \sum_{i \in A} \bar{A}_i(\tau) (\partial_\tau + qJS) A_i(\tau) + \sum_{j \in B} \bar{B}_j(\tau) (\partial_\tau + qJS) B_j(\tau) \right], \end{aligned} \quad (\text{S13})$$

where the terms  $\bar{A}_i \partial_\tau A_i$  and  $\bar{B}_j \partial_\tau B_j$  encode the bosonic Berry phase. Furthermore, we get the retarded interaction,

$$\begin{aligned} \mathcal{S}_{ret} = & - \int \int_0^\beta d\tau d\tau' K(\tau - \tau') \sum_{i \in A} \{ S^2 - S [\bar{A}_i(\tau) A_i(\tau) + \bar{A}_i(\tau') A_i(\tau')] + S [A_i(\tau) \bar{A}_i(\tau') + \bar{A}_i(\tau) A_i(\tau')] \} \\ & - \int \int_0^\beta d\tau d\tau' K(\tau - \tau') \sum_{j \in B} \{ S^2 - S [\bar{B}_j(\tau) B_j(\tau) + \bar{B}_j(\tau') B_j(\tau')] + S [B_j(\tau) \bar{B}_j(\tau') + \bar{B}_j(\tau) B_j(\tau')] \} \end{aligned} \quad (\text{S14})$$

that stems from integrating out the bosons. Note that the diagonal spin-boson interaction leads to an equal-time contribution with a time-dependent correction of  $\mathcal{O}(S^0)$  which we omit, whereas the spin-flip terms lead to a nonlocal interaction in imaginary time. This retarded interaction is mediated by the bath propagator,

$$K(\tau) = \int_0^{\omega_c} d\omega \frac{J(\omega) \cosh[\omega(\beta/2 - \tau)]}{\pi 2 \sinh[\omega\beta/2]}, \quad \text{where} \quad J(\omega) = \begin{cases} 2\pi\alpha J^{1-s} \omega^s & 0 < \omega < \omega_c \\ 0 & \text{else} \end{cases}. \quad (\text{S15})$$

We assume a power-law spectrum  $J(\omega)$  with exponent  $s$  and frequency cutoff  $\omega_c$ , where  $s = 1$  corresponds to an ohmic bath. We have included the Heisenberg exchange constant  $J$  in the definition of  $J(\omega)$  so that the spin-boson coupling  $\alpha$  becomes dimensionless. With this definition,  $K(\tau)$  does not change for  $\omega_c \tau \gg 1$  if we change  $\omega_c$ .

### Diagonalization of the action

In order to diagonalize the action, we define the Fourier transformation of the bosonic fields,

$$A_i(\tau) = \frac{1}{\sqrt{\beta L'}} \sum_{\mathbf{kn}} e^{i(\Omega_n \tau - \mathbf{k} \cdot \mathbf{r}_i)} A_{\mathbf{kn}}, \quad A_{\mathbf{kn}} = \frac{1}{\sqrt{\beta L'}} \int_0^\beta d\tau \sum_{i \in A} e^{-i(\Omega_n \tau - \mathbf{k} \cdot \mathbf{r}_i)} A_i(\tau), \quad (\text{S16})$$

$$B_j(\tau) = \frac{1}{\sqrt{\beta L'}} \sum_{\mathbf{kn}} e^{-i(\Omega_n \tau - \mathbf{k} \cdot \mathbf{r}_j)} B_{\mathbf{kn}}, \quad B_{\mathbf{kn}} = \frac{1}{\sqrt{\beta L'}} \int_0^\beta d\tau \sum_{j \in B} e^{i(\Omega_n \tau - \mathbf{k} \cdot \mathbf{r}_j)} B_j(\tau), \quad (\text{S17})$$

where we introduced the number of sites per sublattice,  $L' = L/2$ , the lattice vector  $\mathbf{r}_i$ , the momentum  $\mathbf{k}$ , and the bosonic Matsubara frequencies  $\Omega_n = 2\pi n/\beta$ ,  $n \in \mathbb{Z}$ . For the Heisenberg interaction, we obtain

$$\mathcal{S}_s = \frac{L\beta qJS^2}{2} + qJS \sum_{\mathbf{kn}} [\gamma_{\mathbf{k}} A_{\mathbf{kn}} B_{\mathbf{kn}} + \gamma_{\mathbf{k}}^* \bar{A}_{\mathbf{kn}} \bar{B}_{\mathbf{kn}}] + \sum_{\mathbf{kn}} [(i\Omega_n + qJS) \bar{A}_{\mathbf{kn}} A_{\mathbf{kn}} + (-i\Omega_n + qJS) \bar{B}_{\mathbf{kn}} B_{\mathbf{kn}}], \quad (\text{S18})$$

where  $\gamma_{\mathbf{k}} = q^{-1} \sum_{\delta} e^{i\mathbf{k} \cdot \delta}$  only depends on the translation vectors  $\delta_1, \dots, \delta_q$  between nearest-neighbor sites. For the retarded interaction, we get

$$\mathcal{S}_{ret} = -L\beta S^2 K_0 + 2S \sum_{\mathbf{kn}} (K_0 - K_n) [\bar{A}_{\mathbf{kn}} A_{\mathbf{kn}} + \bar{B}_{\mathbf{kn}} B_{\mathbf{kn}}]. \quad (\text{S19})$$

Here, we used the Matsubara transformation of the boson propagator,

$$K_n = \int_0^\beta d\tau e^{i\Omega_n \tau} K(\tau) = \int_0^{\omega_c} d\omega \frac{J(\omega)}{\pi} \frac{\omega}{\omega^2 + \Omega_n^2}. \quad (\text{S20})$$

Note that  $K_{-n} = K_n$ . Eventually, the full interaction becomes  $\mathcal{S}_s + \mathcal{S}_{\text{ret}} = L\beta S^2 (qJ/2 - K_0) + \mathcal{S}_1 + \mathcal{O}(S^0)$ , where

$$\mathcal{S}_1 = \sum_{\mathbf{kn}} \begin{pmatrix} \bar{A}_{\mathbf{kn}} & B_{\mathbf{kn}} \\ qJS \gamma_{\mathbf{k}} & -i\Omega_n + qJS + 2S(K_0 - K_n) \end{pmatrix} \begin{pmatrix} A_{\mathbf{kn}} \\ \bar{B}_{\mathbf{kn}} \end{pmatrix}. \quad (\text{S21})$$

The action  $\mathcal{S}_1$  can be diagonalized using the real-valued canonical Bogoliubov transformation

$$\begin{pmatrix} \alpha_{\mathbf{kn}} \\ \bar{\beta}_{\mathbf{kn}} \end{pmatrix} = \begin{pmatrix} u_{\mathbf{k}} & v_{\mathbf{k}} \\ v_{\mathbf{k}} & u_{\mathbf{k}} \end{pmatrix} \begin{pmatrix} A_{\mathbf{kn}} \\ \bar{B}_{\mathbf{kn}} \end{pmatrix}, \quad \begin{pmatrix} A_{\mathbf{kn}} \\ \bar{B}_{\mathbf{kn}} \end{pmatrix} = \begin{pmatrix} u_{\mathbf{k}} & -v_{\mathbf{k}} \\ -v_{\mathbf{k}} & u_{\mathbf{k}} \end{pmatrix} \begin{pmatrix} \alpha_{\mathbf{kn}} \\ \bar{\beta}_{\mathbf{kn}} \end{pmatrix}, \quad (\text{S22})$$

which fulfills  $u_{\mathbf{k}}^2 - v_{\mathbf{k}}^2 = 1$  in order to preserve the measure of the path integral. We determined the matrix elements to be

$$u_{\mathbf{k}} = \sqrt{\frac{1}{2} \left( \frac{1}{\sqrt{1 - w_{\mathbf{k}}^2}} + 1 \right)}, \quad v_{\mathbf{k}} = \sqrt{\frac{1}{2} \left( \frac{1}{\sqrt{1 - w_{\mathbf{k}}^2}} - 1 \right)}, \quad w_{\mathbf{k}} = \frac{qJS |\gamma_{\mathbf{k}}|}{qJS + 2S(K_0 - K_n)}, \quad (\text{S23})$$

such that the action takes the diagonal form

$$\mathcal{S}_1 = \sum_{\mathbf{kn}} [(i\Omega_n + \epsilon_{\mathbf{kn}}) \bar{\alpha}_{\mathbf{kn}} \alpha_{\mathbf{kn}} + (-i\Omega_n + \epsilon_{\mathbf{kn}}) \bar{\beta}_{\mathbf{kn}} \beta_{\mathbf{kn}}], \quad (\text{S24})$$

$$\text{where } \epsilon_{\mathbf{kn}} = \sqrt{[qJS + 2S(K_0 - K_n)]^2 - (qJS)^2 |\gamma_{\mathbf{k}}|^2}. \quad (\text{S25})$$

For  $\alpha = 0$ , we recover the magnon dispersion of the antiferromagnetic Heisenberg model,  $\epsilon_{\mathbf{k}} = qJS \sqrt{1 - |\gamma_{\mathbf{k}}|^2}$ . In one dimension, we have  $\gamma_k = \cos(k)$  such that  $\epsilon_k = 2JS |\sin(k)|$ , i.e., the dispersion is linear at low energies. For any finite spin-boson coupling  $\alpha$ ,  $\epsilon_{\mathbf{kn}}$  shows a nontrivial dependence on the Matsubara frequency and therefore cannot be interpreted as a dispersion relation anymore. To get access to the spectrum, one has to perform the analytic continuation of the Green's function which is proportional to  $1/(\Omega_n^2 + \epsilon_{\mathbf{kn}}^2)$ . Eventually, the spin-boson coupling will lead to a continuous spectral function; this will be discussed elsewhere.

We want to take a closer look at the frequency dependence of  $\epsilon_{\mathbf{kn}}$  in Eq. (S25). To this end, we calculate  $K_n$  using the definitions in Eqs. (S20) and (S15). We find that  $K_0 = 2\alpha J^{1-s} \omega_c^s / s$  diverges with the cutoff frequency. For the ohmic case with  $s = 1$ , we can calculate  $K_n$  for any  $\omega_c$ , i.e.,  $K_n = 2\alpha [\omega_c - \Omega_n \arctan(\omega_c / \Omega_n)]$ . We find that the divergent term in the cutoff frequency drops out such that the limit  $\omega_c \rightarrow \infty$  is well defined. More generally, we have

$$\lim_{\omega_c \rightarrow \infty} (K_0 - K_n) = \frac{\pi \alpha J^{1-s} |\Omega_n|^s}{\sin(\pi s / 2)}, \quad 0 < s < 2, \quad (\text{S26})$$

so that the coupling to the bosonic bath leads to a term proportional to  $|\Omega_n|^s$ .

### Stability of the spin-wave solution

In the following, we want to test whether antiferromagnetic order remains stable within the spin-wave solution. To this end, we calculate the expectation value of the boson occupation number,

$$N_S = \frac{1}{L\beta} \int_0^\beta d\tau \left[ \sum_{i \in A} \langle \hat{A}_i^\dagger(\tau) \hat{A}_i(\tau) \rangle + \sum_{j \in B} \langle \hat{B}_j^\dagger(\tau) \hat{B}_j(\tau) \rangle \right]. \quad (\text{S27})$$

If  $N_S$  diverges, the leading-order fluctuations of the spin-wave solution destroy the antiferromagnetic ground state, whereas the ordered state remains stable as long as  $N_S$  is finite. After transforming this expectation value into the diagonal basis of our path-integral solution, we get (note that we omit a constant shift of  $1/2$ )

$$\begin{aligned} N_S &= \frac{1}{\beta L} \sum_{\mathbf{kn}} (u_{\mathbf{k}}^2 + v_{\mathbf{k}}^2) \langle \bar{\alpha}_{\mathbf{kn}} \alpha_{\mathbf{kn}} + \bar{\beta}_{\mathbf{kn}} \beta_{\mathbf{kn}} \rangle = \frac{1}{\beta L} \sum_{\mathbf{kn}} (u_{\mathbf{k}}^2 + v_{\mathbf{k}}^2) \left[ \frac{1}{i\Omega_n + \epsilon_{\mathbf{kn}}} + \frac{1}{-i\Omega_n + \epsilon_{\mathbf{kn}}} \right] \\ &= \frac{2}{\beta L} \sum_{\mathbf{kn}} \frac{qJS + 2S(K_0 - K_n)}{\Omega_n^2 + \epsilon_{\mathbf{kn}}^2}. \end{aligned} \quad (\text{S28})$$

Now we can take the continuum limit and use of the frequency dependence of  $K_n$  given in Eq. (S26) to obtain

$$N_S = \frac{4}{(2\pi)^{d+1}} \int_0^{\omega_c} d\omega \int_{\text{BZ}} d\mathbf{k} \frac{qJS + \tilde{\alpha}\omega^s}{\omega^2 + [qJS + \tilde{\alpha}\omega^s]^2 - (qJS)^2 |\gamma_{\mathbf{k}}|^2}, \quad (\text{S29})$$

where we have gained a factor of 2 because the integrand is an even function in  $\omega$ . Furthermore, we defined  $\tilde{\alpha} = 2\pi\alpha S J^{1-s} / \sin(\pi s/2)$ . For the one-dimensional case, the integral becomes

$$N_S = \frac{1}{\pi^2} \int_0^{\omega_c} d\omega \int_0^{2\pi} dk \frac{2JS + \tilde{\alpha}\omega^s}{\omega^2 + 2JS \sin^2(k) + 4JS\tilde{\alpha}\omega^s + \tilde{\alpha}^2\omega^{2s}} \quad (\text{S30})$$

$$= \frac{2}{\pi} \int_0^{\omega_c} d\omega \frac{2JS + \tilde{\alpha}\omega^s}{2JS\sqrt{(\omega^2 + 4JS\tilde{\alpha}\omega^s + \tilde{\alpha}^2\omega^{2s})(1 + \omega^2 + 4JS\tilde{\alpha}\omega^s + \tilde{\alpha}^2\omega^{2s})}}. \quad (\text{S31})$$

In the last step, we have used  $\int_0^{2\pi} dk [a + \sin^2(k)] = 2\pi/\sqrt{a(1+a)}$ .

Now we want to determine whether  $N_S$  diverges or remains finite. To this end, we analyze the low-frequency limit of the integrand in Eq. (S31). The leading behavior is determined by  $1/\sqrt{\omega^2 + c\alpha\omega^s}$ . For  $\alpha = 0$ , it becomes  $1/\omega$  and therefore the integral diverges. However, for any finite coupling to the bath, the leading behavior becomes  $1/\sqrt{\omega^s}$  which is integrable for  $s < 2$ . As a result, the coupling to the bath stabilizes long-range antiferromagnetic order for large  $S$ .

Finally, from Eq. (S30) we can also deduce that conformal invariance is broken by the coupling to the bath. For  $\omega \ll 1$  and  $k \ll 1$ , the propagator becomes  $1/(\omega^2 + v_s^2 k^2 + \alpha'\omega^s)$  where  $v_s$  corresponds to the spin-wave velocity. Hence, we have  $z = 2$  for the coupling to an ohmic bath with  $s = 1$ .

## SCALING OF THE LOCAL SUSCEPTIBILITY FOR THE HEISENBERG CHAIN

At zero temperature and in the thermodynamic limit, the Lorentz symmetry inherent to the Heisenberg spin chain leads to

$$\langle \hat{S}^z(r, \tau) \hat{S}^z(0, 0) \rangle \propto \frac{1}{\sqrt{r^2 + (v_s \tau)^2}}. \quad (\text{S32})$$

Here,  $v_s$  corresponds to the spin-wave velocity and we have omitted logarithmic corrections. If we now consider a finite-sized system of length  $L$ , the system will have a spin gap set by  $\Delta_s = v_s 2\pi/L$ . Hence,

$$\langle \hat{S}^z(r=0, \tau) \hat{S}^z(0, 0) \rangle \propto \begin{cases} \frac{1}{v_s \tau} & \text{if } \tau \Delta_s < 1 \\ \frac{\Delta_s}{v_s} e^{-\tau \Delta_s} & \text{if } \tau \Delta_s > 1 \end{cases}. \quad (\text{S33})$$

Then, the local spin susceptibility in the zero-temperature limit and for a finite system size reads

$$\int_0^\infty d\tau \langle \hat{S}^z(r=0, \tau) \hat{S}^z(0, 0) \rangle \propto \ln(L). \quad (\text{S34})$$

Since space and time are interchangeable for Lorentz-invariant systems, similar arguments can be put forward to show that the local susceptibility at finite temperatures and in the thermodynamic limit scales as  $\ln(\beta)$ .